

Bridging steady states with renormalization group analysis

Yueheng Lan*

Department of Physics, Tsinghua University, Beijing 100084, China

(Received 27 October 2012; revised manuscript received 19 November 2012; published 25 January 2013)

Transitions between different condensed phases, molecular conformations, chemical compositions, or spatiotemporal patterns play important roles in many branches of natural science and at the same time incur serious challenges in their precise characterization. We design an approach for computing connecting orbits bridging steady states based on the renormalization group analysis. The technique is successfully applied to several interesting examples and good analytic results are obtained in a systematic and unified way.

DOI: [10.1103/PhysRevE.87.012914](https://doi.org/10.1103/PhysRevE.87.012914)

PACS number(s): 05.45.-a, 05.10.Cc, 02.30.Mv, 02.70.-c

I. INTRODUCTION

Transitions between different steady states always make a central part of system dynamics and are key to the understanding of many interesting physical, chemical, or biological processes. From a dynamical systems point of view, they are all described by connections that link equilibria in the state space. Instantons in quantum mechanics, solitary waves in shallow water dynamics, propagating fronts in combustion problems, and chemical reaction paths in the transition state theory are all closely related to these connecting orbits [1–4], among which the heteroclinic ones often guide the transition from one state to another. The nonequilibrium dynamics globally can be viewed as a directed graph with vertices being the local steady states and edges being the connecting orbits. The embedded network structure of state transitions has been observed in many systems, ranging from spatiotemporally chaotic fluids to a folding protein [5–10]. How to find these connections and determine their properties constitute an important part of understanding global properties of heterogeneous, strongly interacting, multiagent systems.

The most popular way of locating a connecting orbit is through numerical computation [11–15]. Analytical approximation can sometimes be obtained with the help of asymptotic analysis [16]. Both methods require the knowledge of the steady states at both ends and dynamics in their neighborhoods. Very rarely, an exact solution may be obtained through skilled and involved analytical manipulation [17–19]. Although much progress has been made, in general, the detection and analysis of connecting orbits remains a challenge for researchers in both mathematics and natural sciences, which await new tools for an elegant solution.

The renormalization group (RG) method was first proposed in theoretical physics for removing singularities in the perturbation theory of quantum physics [20]. The idea was extended to the asymptotic analysis of differential equations not long ago [21,22]. Compared to the traditional asymptotic methods, it is simple to use and has the potential to accommodate most of the existing analysis. Much work has been done to illuminate its mathematical significance and to simplify its solution procedure. Until now, the method has been widely tested in various systems and often proved to be very effective [21,23–27].

Previous RG schemes often result in nonlinear equations of the same dimension as the original one. Here, we generalize the method to the detection of one-dimensional orbits that connect different steady states. A restrained RG scheme was designed in literature to determine the center manifold and the dynamics on it [28] or hyperbolic invariant manifolds with certain constraints on the spectrum of the linearized equation [29]. The method to be explained here has no such constraints and works for general parameter values. It also has the advantage that only one end point is needed in the analysis and the other end point can be determined by the resulting RG equation. Therefore, exploration of a high-dimensional phase space could be concentrated on its one-dimensional foliations by the RG analysis, which will provide great convenience for studying transitions in many physical systems. Moreover, an analytical approximation is easily computed with the RG approach and exact solutions may even be obtainable occasionally.

In this paper, we apply the new RG method to the determination of heteroclinic orbits in differential systems. Below is the organization of the rest of the paper. After an explanation of the RG method and our generalization in Sec. II, we will apply it to three typical examples in Sec. III: the Lotka-Volterra model of competition in ecology [30], the Gray-Scott model in chemical reaction kinetics [18], and the Kuramoto-Sivashinsky equation [31–33] that describes spatiotemporal pattern formation. All these systems have different characteristics and will be used to show interesting aspects of the RG method. In Sec. IV, the findings will be summarized and possible future development and applications will be mentioned.

II. RENORMALIZATION GROUP METHOD FOR DIFFERENTIAL EQUATIONS

Here, we will explain how the RG is applied to the solution of differential equations and what our extension is. Suppose that we have a set of n -dimensional differential equation

$$\dot{\mathbf{x}} = L\mathbf{x} + \epsilon N(\mathbf{x}), \quad (1)$$

where $\mathbf{x} = (x_1, x_2, \dots, x_n)^t \in \mathbb{R}^n$ and L is an $n \times n$ matrix. $N(\mathbf{x}) \sim O(|\mathbf{x}|^2)$ is the nonlinear term which is assumed to be analytic in the neighborhood of $\mathbf{x} = 0$. ϵ is a small parameter which signifies the magnitude of the nonlinear term. Suppose L is diagonalizable, e.g., $L = \text{diag}(\lambda_1, \lambda_2, \dots, \lambda_n)$ a diagonal

*lanyh@mail.tsinghua.edu.cn

matrix, where λ_i 's are eigenvalues of L . Below, we will first make a naive expansion and then derive the RG equation.

We may make the expansion

$$\mathbf{x} = \mathbf{u}_0 + \epsilon \mathbf{u}_1 + \epsilon^2 \mathbf{u}_2 + \dots \quad (2)$$

By substituting Eq. (2) into Eq. (1) and comparing different orders of ϵ , we obtain

$$\begin{aligned} \dot{\mathbf{u}}_0 &= L\mathbf{u}_0 \\ \dot{\mathbf{u}}_1 &= L\mathbf{u}_1 + N(\mathbf{u}_0) \\ \dot{\mathbf{u}}_2 &= L\mathbf{u}_2 + N_2(\mathbf{u}_0, \mathbf{u}_1) \\ &\dots \end{aligned} \quad (3)$$

where $N_2(\mathbf{u}_0, \mathbf{u}_1) = \nabla N(\mathbf{u}_0) \cdot \mathbf{u}_1$ denotes the second order nonlinear driving. The first equation in Eq. (3) is linear and its solution is

$$\mathbf{u}_0(t, t_0) = e^{L(t-t_0)} \mathbf{A}, \quad (4)$$

where $\mathbf{A} = \mathbf{A}(t_0)$ is a constant vector of integration and t_0 is the initial time, which upon a substitution into the second equation of Eq. (3) results in

$$\mathbf{u}_1(t, t_0) = e^{L(t-t_0)} \int_{t_0}^t e^{-L(\tau-t_0)} N[e^{L(\tau-t_0)} \mathbf{A}] d\tau, \quad (5)$$

where $\mathbf{u}_1(t_0, t_0) = 0$ has been assumed for convenience. With L being diagonal, each component of $\mathbf{u}_1(t, t_0)$ may be computed separately. The integration in Eq. (5) gives exponential functions unless resonance terms happen to exist, in which case powers of $(t - t_0)$ will appear.

In a similar way, higher-order terms such as $\mathbf{u}_2, \mathbf{u}_3$ may be computed. Substituting these results into Eq. (2), we get the naive perturbation expansion. If all the eigenvalues of L satisfy $\text{Re}(\lambda_i) \leq 0$, then this expansion can be very efficient unless there are resonances which bring in the powers of $t - t_0$ and invalidate the perturbation expansion when $t - t_0$ is not small. We need the RG technique to get better approximation. The series expansion Eq. (2) gives $\mathbf{x} = \tilde{\mathbf{x}}[t; t_0, \mathbf{A}(t_0)]$. The RG equation is a set of equations for $d\mathbf{A}(t_0)/dt_0$, which can be derived from the renormalization equation [21,34]

$$\left. \frac{d\tilde{\mathbf{x}}[t; t_0, \mathbf{A}(t_0)]}{dt_0} \right|_{t=t_0} = 0. \quad (6)$$

If $\tilde{\mathbf{x}}[t; t_0, \mathbf{A}(t_0)]$ is an exact solution, the resulting evolution equation for $\mathbf{A}(t_0)$ is also exact. An order ϵ^m approximation for $d\mathbf{A}(t_0)/dt_0$ is derived if $\tilde{\mathbf{x}}[t; t_0, \mathbf{A}(t_0)]$ is accurate up to order ϵ^m [25]. Note that this statement is true as long as t is close to t_0 . Once the equation for $\mathbf{A}(t_0)$ is solved, the solution of the original equation, Eq. (1), can be well approximated by $\mathbf{x}(t_0) \approx \tilde{\mathbf{x}}[t_0; t_0, \mathbf{A}(t_0)]$. The nice feature of this form of solution is that the substitution $t \rightarrow t_0$ removes the divergent resonance terms.

Note that Eq. (6) is linear in the n unknowns $d\mathbf{A}(t_0)/dt_0$, which can easily be computed from the n equations. We are mostly interested in the dynamics on a submanifold, which may be described by less than n independent variables. As a consequence, less than n free parameters $\mathbf{A}(t_0)$ is at our disposal due to the constraint. If previous strategy is used to arrive at a similar equation to Eq. (6), an awkward situation arises that there are more equations than unknowns. When a center manifold exists and all eigenvalues have nonpositive real

parts, a certain scheme is designed to adapt the RG technique to the description of the dynamics on the manifold [35]. Below, we are going to introduce a new strategy to derive the RG equation on a generic invariant submanifold. Without loss of generality, we will concentrate on the 1D submanifold. Higher-dimensional ones can be treated in a similar way.

Suppose that we are interested in the dynamics on the submanifold corresponding to the eigenvalue λ_1 , lying in the x_1 direction in an infinitesimal neighborhood of the origin. Then the initial vector \mathbf{A} should be taken as $\mathbf{A} = (A_1, 0, 0, \dots, 0)^t$; i.e., only the first component is retained. Subsequent iterations for higher-order terms in the series Eq. (2) remain the same for the first component but have to be modified for others. As an example, the i th ($i \neq 1$) component of \mathbf{u}_1 can be computed as

$$u_{1,i}(t, t_0) = e^{\lambda_i(t-t_0)} \int_{t_0}^t e^{-\lambda_i(\tau-t_0)} N(e^{L(\tau-t_0)} \mathbf{A}) d\tau, \quad (7)$$

where \int^t denotes integration without a constant term. As mentioned before, the integration result should be exponential or power functions of $t - t_0$. This integration strategy can be easily applied to higher-order terms.

In the approximate solution series Eq. (2), only one constant A_1 is at our disposal, so that we cannot directly use Eq. (6) any longer. In fact, we may use its first component,

$$\left. \frac{d\tilde{x}_1[t; t_0, A_1(t_0)]}{dt_0} \right|_{t=t_0} = 0, \quad (8)$$

to derive the RG equation for $dA_1(t_0)/dt_0$. How about other component equations? Surprisingly, they are all satisfied by the solution of this one RG equation!

The assertion can be proven by mathematical induction. According to Eq. (1) and our integration procedure Eq. (7), it is easy to write down an integral equation for its i th ($i \neq 1$) component:

$$x_i[t; t_0, A_1(t_0)] = \epsilon e^{\lambda_i(t-t_0)} \int_{t_0}^t e^{-\lambda_i(\tau-t_0)} N\{\mathbf{x}[\tau; t_0, A_1(t_0)]\} d\tau. \quad (9)$$

Suppose that Eq. (6) is satisfied up to order ϵ^m for every component with a solution of $dA_1(t_0)/dt_0$ accurate up to order ϵ^m . We may take t_0 derivatives on both sides of Eq. (9) and impose $t \rightarrow t_0$

$$\begin{aligned} &\frac{\partial x_i[t; t_0, A_1(t_0)]}{\partial t_0} \\ &= \epsilon \int_{t_0}^t e^{-\lambda_i(\tau-t_0)} \nabla N\{\mathbf{x}[\tau; t_0, A_1(t_0)]\} \frac{\partial \mathbf{x}[\tau; t_0, A_1(t_0)]}{\partial t_0} d\tau \\ &\sim O(\epsilon^{m+1}). \end{aligned} \quad (10)$$

That is, Eq. (6) is satisfied up to order ϵ^{m+1} for $i \neq 1$. For $i = 1$, we directly solve the first component of Eq. (6) for $dA_1(t_0)/dt_0$ with the accuracy of order ϵ^{m+1} . So, for this particular solution of $dA_1(t_0)/dt_0$, Eq. (6) is satisfied up to order ϵ^{m+1} . It is easy to check that our assertion is true for $m = 1$. By induction, it is true for all values of m .

In the current paper, we do not prove the convergence of the solution series. However, in Chiba's recent papers [28,29], the convergence of the RG method and the diffeomorphism of the compact normally hyperbolic invariant manifold

between the approximate and the exact dynamics are proven for sufficiently small ϵ under quite general conditions.

III. APPLICATIONS

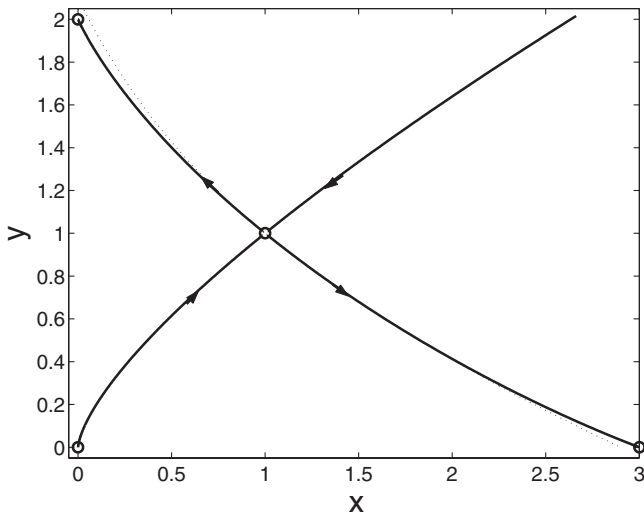
Below, the new method is applied to three examples that are specifically chosen because they demonstrate different aspects of the method: one from biophysics—the Lotka-Volterra model of competition; one from chemical physics—the Gray-Scott model of cubic autocatalytic chemical reactions; and one from pattern formation study—the Kuramoto-Sivashinsky equation. In the first example, the RG technique determines both the end points and the connections of a nonlinear ODE at the same time with the knowledge of the starting point. The second example shows that the method is applicable to systems with multiple stable and unstable directions, and it is even possible to obtain exact solutions through the RG analysis. The third example shows that the current RG computation can be easily applied to spatially extended systems. In addition to the three examples presented here, the method has been applied to quite a few other examples, including Lorenz equation with equal success, which shows its general validity.

A. The Lotka-Volterra model of competition

Here, we use the classic Lotka-Volterra model of competition as an example to explain our technique. The model describes the competition between the rabbits and the sheep fed on the grass of the same lawn. Each species would follow a logistic growth in the absence of the other, but the competition for food occurs when a rabbit meets a sheep. Mathematically, the model can be expressed as

$$\begin{aligned}\dot{x} &= x(3 - x - 2y) \\ \dot{y} &= y(2 - x - y),\end{aligned}\quad (11)$$

where x, y are the rabbit number and the sheep number, respectively.



Equation (11) has four equilibria $P_1 = (0,0)$, $P_2 = (0,2)$, $P_3 = (1,1)$, $P_4 = (3,0)$. Five connecting orbits exist between these points, but it seems hard to obtain exact analytic expressions for orbits connecting to the saddle point P_3 . Numerical computation give the three heteroclinic orbits that connect P_3 to other equilibria, shown in Fig. 1(a) (solid line).

In fact, the RG technique can be effectively used to give analytic approximations of these heteroclinic orbits. To study the behavior of Eq. (11) around the saddle P_3 , we take a coordinate transformation $x = 1 - \sqrt{\frac{2}{3}}z + \sqrt{\frac{2}{3}}w$, $y = 1 + \sqrt{\frac{1}{3}}z + \sqrt{\frac{1}{3}}w$, such that the stable and the unstable directions of P_3 go along the z and the w axis. Next, we carry out the usual perturbative expansion procedure by first assuming

$$\begin{aligned}z &= \epsilon z_1 + \epsilon^2 z_2 + \epsilon^3 z_3 + \dots, \\ w &= \epsilon w_1 + \epsilon^2 w_2 + \epsilon^3 w_3 + \dots\end{aligned}\quad (12)$$

and substituting it into the equation satisfied by $z(t)$ and $w(t)$. By a comparison of different orders of ϵ , we have

$$\begin{aligned}\mathcal{L} \circ z_1 &\equiv \left(1 - \sqrt{2} + \frac{d}{dt}\right) z_1 = 0 \\ \mathcal{M} \circ w_1 &\equiv \left(1 + \sqrt{2} + \frac{d}{dt}\right) w_1 = 0\end{aligned}\quad (13)$$

$$\begin{aligned}\mathcal{L} \circ z_2 &= F_2(z_1, w_1) \\ \mathcal{M} \circ w_2 &= G_2(z_1, w_1)\end{aligned}\quad (14)$$

$$\dots, \quad (15)$$

where F_2, G_2 are polynomial functions of their arguments. The linear operators \mathcal{L}, \mathcal{M} are defined in Eq. (13) and keep popping up in later equations. The general solution of Eq. (13) is

$$z_1(t) = a(t_0)e^{(\sqrt{2}-1)(t-t_0)}, \quad w_1(t) = b(t_0)e^{-(1+\sqrt{2})(t-t_0)}, \quad (16)$$

where $[a(t_0), b(t_0)]$ is the initial position. Here comes the leap. With a suitable choice of the initial position, we may stay on a submanifold. For example, if we set $b(t_0) = 0$, then we will work on the unstable manifold of the original saddle P_3 , which

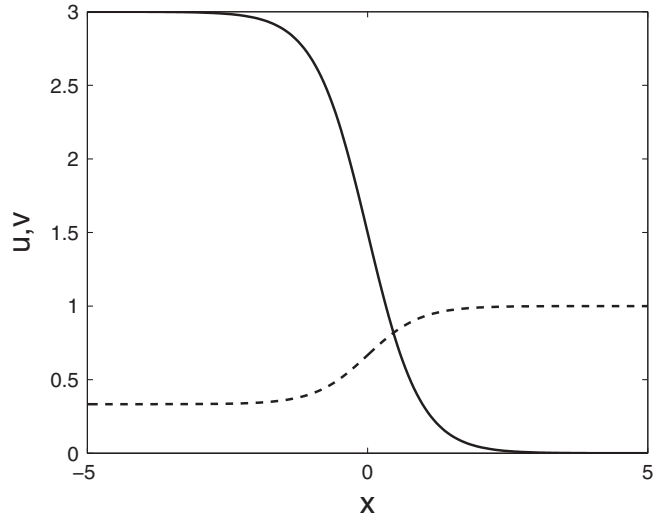


FIG. 1. The connecting orbits in (a) the Lotka-Volterra model (solid lines, the true heteroclinic orbits; dotted lines, the heteroclinic orbits obtained through RG) and (b) the Gray-Scott model.

is one-dimensional. Substituting this solution into Eq. (14), we get a solution of z_2 , w_2 , again with two arbitrary constants, which could be chosen such that $z_2(t_0) = 0$ and that no terms proportional to $\exp[-(1 + \sqrt{2})(t - t_0)]$ appear. Repeating this process, we get approximations of higher orders:

$$z = \epsilon a(t_0) e^{(\sqrt{2}-1)(t-t_0)} + \frac{\sqrt{3}\epsilon^2 a^2(t_0)}{6} (\sqrt{2}-1) \times [e^{2(\sqrt{2}-1)(t-t_0)} - e^{(\sqrt{2}-1)(t-t_0)}] + \dots \quad (17)$$

$$w = \frac{\sqrt{3}\epsilon^2 a^2(t_0)}{102} (1 + 3\sqrt{2}) e^{2(\sqrt{2}-1)(t-t_0)} + \dots \quad (18)$$

Following the standard procedure, we take derivative of Eq. (17) with respect to t_0 and let $t \rightarrow t_0$, arriving at an equation for $da(t_0)/dt_0$, which results in

$$\frac{da(t_0)}{dt_0} = a \left[\sqrt{2} - 1 - \frac{17\sqrt{3}(3-2\sqrt{2})}{102} \epsilon a - \frac{7+4\sqrt{2}}{102} \epsilon^2 a^2 \right]. \quad (19)$$

Similar result may be obtained from Eq. (18), which justifies the consistency of our scheme. So, from the commonly used local perturbation series expansion Eq. (12), an RG equation for the amplitude is obtained. The strength of Eq. (19) is that it captures well the dynamics of the original Eq. (11) in an much extended region. This can be clearly seen in comparison with numerical computation results though rigorous proofs like those given by Chiba [28,29] are still lacking. Through application to different systems, we found that this practice seems valid in the case that the connecting orbit is not geometrically intricate.

With $\epsilon = 1$, Eq. (19) has three stationary points, $a_1 \approx 0$, $a_2 \approx -2.037$, $a_3 \approx 1.638$, which can be transformed back to $(1,1)$, $(2.908, -0.003)$, $(-0.113, 2.105)$ in the original x - y phase space, apparently corresponding to the equilibria P_3 , P_4 , P_2 , respectively. Considering this fairly low order of the approximation, the five percent error in the position is not bad. If we use higher-order approximation, more accurate results can be achieved. In Fig. 1(a), these equilibria plus P_1 are marked with circles. The approximate heteroclinic connections (dotted line) obtained with the RG procedure are seen to be very close to the true ones (solid line). Moreover, an analytic approximation of the connections can be obtained by solving Eq. (19) with quadrature, if necessary. Therefore, through the RG, we can approximate very well the heteroclinic connections and the dynamics on them.

B. The Gray-Scott model

The Gray-Scott model represents the cubic autocatalytic chemical reactions for two chemical species A and B , which take place in a confined region of space [18]: $\Phi \rightarrow A$, $A + 2B \rightarrow 3B$, $B \rightarrow C$. The stationary patterns are described by the following equations:

$$\begin{aligned} u'' &= uv^2 - \lambda(1-v) \\ \gamma v'' &= v - uv^2, \end{aligned} \quad (20)$$

where u, v are concentrations of the two chemicals A, B in a dimensionless form. The primes represent spatial derivatives d/dx . Equation (20) has two heteroclinic orbits when $\gamma = 2/9$ and $\lambda = 9/2$. At this parameter value, Eq. (20) has three equilibria, $P_1 = (1,0)$, $P_2 = (1/3,3)$, $P_3 = (2/3,3/2)$, and we will discuss the possible connections between P_1 and P_2 . In fact, the phase space of Eq. (20) is 4D. If we introduce $p = u'$, $w = v'$, then the 4D dynamical system is

$$\begin{aligned} u' &= p, & p' &= uv^2 - \lambda(1-v), \\ v' &= w, & w' &= v - uv^2. \end{aligned} \quad (21)$$

A perturbation expansion is carried out around the equilibrium P_1 . Equation (21) at P_1 possesses linear stability exponents $\pm 3\sqrt{2}/2$, both being doubly degenerate, which suggests that the equilibrium P_1 has a 2D stable and a 2D unstable manifold. We may work on the stable manifold and have to use two parameters, $r_0(x_0)$, r_1 , to parametrize the initial position, where r_1 is used to select the filament that embeds the heteroclinic connection on the 2D stable surface and $r_0(x_0)$ is used to parametrize the connection.

The remaining two arbitrary parameters in solution of the ϵ^1 equation are used to remove terms proportional to $\exp(3\sqrt{2}/2t)$. In the solution of the later higher-order equations, two of the four arbitrary parameters in each order are used to do this removal and the other two are used to keep $u_n(x_0) = 0$, $v_n(x_0) = 0$ for $n \geq 2$. With these considerations, we obtain

$$\begin{aligned} u &= 1 + \epsilon \left(-\frac{\sqrt{2}r_0 f(x, x_0)}{3} \right) \\ &\quad + \epsilon^2 \frac{4}{243} [f^2(x, x_0) - f(x, x_0)] r_0^2 r_1^2 + \dots \\ p &= \epsilon f(x, x_0) r_0 - \epsilon^2 \frac{2\sqrt{2}}{81} [2f^2(x, x_0) - f(x, x_0)] r_0^2 r_1^2 + \dots \\ v &= \epsilon \left(-\frac{\sqrt{2}r_0 r_1 f(x, x_0)}{3} \right) \\ &\quad - \epsilon^2 \frac{2}{27} [f^2(x, x_0) - f(x, x_0)] r_0^2 r_1^2 + \dots \\ w &= \epsilon f(x, x_0) r_0 r_1 - \epsilon^2 \frac{\sqrt{2}}{9} [2f^2(x, x_0) - f(x, x_0)] r_0^2 r_1^2 + \dots, \end{aligned} \quad (22)$$

where

$$f(x, x_0) = \exp \left[-\frac{3\sqrt{2}}{2} (x - x_0) \right]$$

is the generic linear contraction on the stable manifold.

The RG equation for $r_0(x_0)$ is given by setting $\partial u(x, x_0)/\partial x_0 = 0$ followed by taking $x \rightarrow x_0$, where $u(x, x_0)$ is the first of Eq. (22). By solving the resulting equation, we obtain

$$\begin{aligned} \frac{dr_0(x_0)}{dx_0} &= -\frac{3}{\sqrt{2}} r_0 + \frac{2}{27} \epsilon r_0^2 r_1^2 + \frac{r_0}{21870} \\ &\quad \times [-45\sqrt{2}r_1^2(9+2r_1)\epsilon^2 r_0^2 + 8r_1^3(9+2r_1)\epsilon^3 r_0^3] \\ &\quad + \dots \end{aligned} \quad (23)$$

Here comes a very interesting observation: if we set $r_1 = -9/2$ in Eq. (23), all the terms of order higher than ϵ^1 vanish! In fact, this statement can be easily proved by going to a few higher-order terms. So, by setting $r_1 = -9/2$, we sit on the right filament for the connection, which is described exactly by the following equation (with $\epsilon = 1$):

$$\frac{dr_0(x_0)}{dx_0} = -\frac{3}{\sqrt{2}}r_0 + \frac{3}{2}r_0^2. \quad (24)$$

Similar equations could be obtained if any other component of Eq. (22) was used for the derivation. The 1D dynamical system Eq. (24) has a stable fixed point $r_0 = 0$ and an unstable fixed point $r_0 = \sqrt{2}$, corresponding to the equilibria P_1, P_3 , respectively.

It is easy to solve Eq. (24) to arrive at

$$r_0(x_0) = \frac{\sqrt{2}}{2} \left(1 - \tanh \frac{3x_0}{2\sqrt{2}} \right), \quad (25)$$

where we have fixed the arbitrary constant in the integration. Therefore, utilizing Eq. (22), an exact analytic solution of Eq. (20) is obtained

$$\begin{aligned} u(x) &= 1 - \frac{\sqrt{2}}{3}r_0(x) = \frac{1}{3} \left(2 + \tanh \frac{3x}{2\sqrt{2}} \right) \\ v(x) &= \frac{3}{\sqrt{2}}r_0(x) = \frac{3}{2} \left(1 - \tanh \frac{3x}{2\sqrt{2}} \right). \end{aligned} \quad (26)$$

Due to the time reversal invariance of Eq. (20), the inversion $x \rightarrow -x$ in the solution Eq. (26) gives a second heteroclinic connection with the opposite direction.

In Fig. 1(b), the spatial profiles of the two stationary solutions $u(x), v(x)$ are shown. The concentration of the two chemical species is localized to different parts of the available space.

C. The Kuramoto-Sivashinsky equation

The Kuramoto-Sivashinsky equation was first derived as a generic phase equation for nonlinearly coupled oscillators [32] and also describes a plethora of physics phenomena [33,36–38]. It is a paradigm for studying nonlinear dynamics involving the spatial degrees of freedom [39–41]. An interesting one-dimensional version of it could be written as

$$u_t = (u^2)_x - u_{xx} - \nu u_{xxx}, \quad (27)$$

where $\nu > 0$ is the super-viscosity parameter. Equation (27) is invariant under the transformation $x \rightarrow -x, u \rightarrow -u$. If periodic solutions on the interval $x \in [0, 2\pi]$ are considered, we may use the Fourier representation

$$u(t, x) = i \sum_{k=-\infty}^{\infty} a_k e^{ikx}. \quad (28)$$

For the antisymmetric solution $u(t, -x) = -u(t, x)$, a_k is real and $a_{-k} = -a_k$. In this antisymmetric solution space, the Kuramoto-Sivashinsky equation becomes

$$\dot{a}_k = (k^2 - \nu k^4)a_k - k \sum_{m=-\infty}^{\infty} a_m a_{k-m}. \quad (29)$$

We may use only a_k with $k > 0$ as the state variable.

We are about to study the behavior of Eq. (29) in the neighborhood of the origin—the trivial equilibrium. If $\nu \geq 1$, it can be proved that the origin is a global attractor of Eq. (29). When ν goes below 1, a supercritical bifurcation occurs in the direction of the Fourier component a_1 , where two equilibria are born and connected to the origin through a heteroclinic orbit. We would like to derive an analytic expression of the newly born equilibria and the heteroclinic orbit with the RG analysis.

As before, we first do the usual perturbation analysis by assuming

$$a_k = \epsilon a_{k,1} + \epsilon^2 a_{k,2} + \epsilon^3 a_{k,3} + \dots \quad (30)$$

The substitution of Eq. (30) into Eq. (29) results in a hierarchy of equations for $a_{k,n}$ by comparing different orders of ϵ . As before, if we are only interested in the 1D unstable manifold of the origin when $\nu < 1$, we may set

$$a_{1,1}(t, t_0) = r(t_0)e^{(1-\nu)(t-t_0)}, \quad a_{k,1} = 0 \quad \text{for } k > 1, \quad (31)$$

where $r(t_0)$ is the renormalization parameter. When solving for $a_{k,n}$ with $n \geq 2$, the arbitrary constants are determined by imposing two conditions: (1) $a_{1,n} = 0$; (2) only integer powers of $\exp[(1-\nu)(t-t_0)]$ are admitted in the solution. The RG equation (with $\epsilon = 1$) for $r(t_0)$ is obtained from $da_1(t, t_0)/dt|_{t=t_0} = 0$:

$$\frac{dr_0}{dt_0} = (1-\nu)r_0 + \frac{2r_0^3}{1-7\nu} - \frac{6r_0^5}{(1-7\nu)^2(-1+13\nu)} + \dots \quad (32)$$

From Eq. (32), it is easy to see that when $\nu > 1$, $r_0 = 0$ is the only fixed point, which is stable. At $\nu = 1$, a supercritical bifurcation happens at which the connecting orbit is born. However, as shown in Fig. 2(a), even at the parameter value $\nu = 0.5$, which already deviates quite far away from the bifurcation point, the RG approximation (circles) seems to match the benchmark numerical solution (solid line) very well. The 1D manifold makes a nontrivial curve in the phase space. Also, the magnitude of the Fourier components seems to decrease very rapidly with increasing wave number, which validates our computation with only a few modes and is attributed to the ironing effect of the fourth-order damping term in Eq. (27). Figure 2(b) portrays the time evolution of the physical variable $u(x, t)$. As the uniform solution is not stable any longer, the solution leaves for a spatially modulated

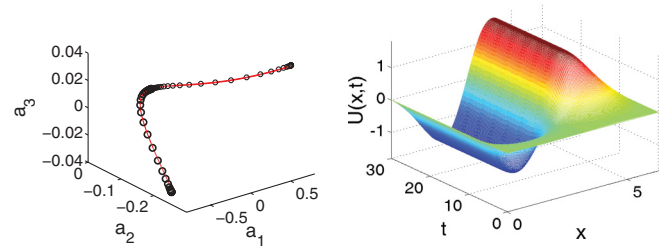


FIG. 2. (Color online) The heteroclinic connections in the Kuramoto-Sivashinsky Eq. (27) at $\nu = 0.5$ represented (a) by the projection onto the first three Fourier modes and (b) by the time evolution of the physical variable $u(x, t)$. The solid lines mark the true heteroclinic orbits and the circles depict the heteroclinic orbits obtained through RG.

pattern dominated by a sinusoidal function. In principle, both the final steady state and the evolution can be approximated analytically with our RG equation.

IV. SUMMARY

In this paper, an extension of the RG method is proposed and successfully used for the determination of connecting orbits in the phase space. The new scheme concentrates on the RG analysis of dynamics on the 1D submanifold, and the resulting RG equation is proved to be consistent among all components of the vector field. The method was applied to three typical physical systems: the Lotka-Volterra model of competition, the Gray-Scott model, and the Kuramoto-Sivashinsky equation. In the first model, the RG equation is derived around a saddle and the other equilibrium and dynamics on it is computed with good precision. In the second example, an exact solution is derived in spite of the occurrence of degenerate eigendirections. The last model is a nonlinear partial differential equation that possesses an infinite-dimensional phase space. The RG method is able to well describe the transition from a homogeneous state to a spatially modulated state despite the high dimensionality. From all these examples, it is reasonable to believe that this RG scheme should be able to be applied to other strongly nonlinear heterogeneous systems and to the study of state transition.

The convergence property of the solution series determines the validity and quality of our finite RG expansion truncation. In our first example, if the RG equation is kept only to the first order, the result would be incorrect. Apparently, a first-order approximation is not enough to represent the whole connecting orbit and the associated dynamics, though it is still valid near the origin $a = 0$. In the examples we tried, second- or third-order approximation usually gives good representation of the orbit. Higher-order approximation often leads to higher accuracy. Still, in our first example, the third-order approximation gives $(-0.07, 2.04)$ as the coordinate of P_2 as compared to $(-0.113, 2.105)$ in the second-order approximation. The third-order approximation also generates a fake fixed point. However, it is far away from the origin and the expansion loses its validity there. The two points that are immediate neighbors of the origin continue to give good approximation. Therefore, a qualitative knowledge of the orbit structure in phase space provides much convenience and guidance for the application of the current RG technique.

In our series solution of the nonlinear equation, we have adopted a particular set of initial conditions, which serves mainly to simplify the later arguments and is by no means unique. As a matter of fact, there is much room left for us to choose the form of the series solution that is most suitable to a particular problem. However, the number of free parameters should be determined by the dimension of the submanifold and is independent of the choice of the series solution. With this freedom, the RG equation and the final form of the solution could be different for different choices, which may be good to represent different solution curves. One thing to be noticed is that in our scheme secular terms might not appear in the naive series solution.

Still there are problems that await a solution. In all these examples, the eigenvalue of the linearized dynamics associated with the connecting orbit has no imaginary part; i.e., the solution is nonoscillatory. Only in this case is the 1D approximation of the dynamics a valid representation. In practice, many connecting orbits approach the steady state in an oscillatory way. How to adapt the current scheme to treating oscillatory orbits is an interesting problem. Also, in all the above examples except the second one, the eigen-directions corresponding to the connection were known *a priori*. We still do not have much of an idea what to do if this information is missing. The second example may give a hint, but more systematic techniques are needed in order to treat the general case. In all the examples, the asymptotic states are equilibria, while connecting orbits may exist between other higher-dimensional invariant sets, such as periodic orbits, invariant tori, or even strange attractors. Further extension of the current RG technique is needed to accommodate all these different cases.

There seems no obstacles to generalize the current technique to the treatment of dynamics on invariant submanifolds of dimensions higher than one. The argument in Sec. II can be similarly applied to the derivation of the RG equation. This may enable systematic and efficient dynamics reduction or approximation of invariant submanifold in many nonlinear systems that appear in various branches of natural science. According to Ref. [26], the method can also be extended to the treatment of discrete dynamics.

ACKNOWLEDGMENT

This research is supported by The Ph.D. Program Foundation of Ministry of Education of China (Grant No. 20090002120054).

-
- [1] E. Infeld and G. Rowlands, *Nonlinear Waves, Solitons, and Chaos* (Cambridge, New York, 1990).
 - [2] R. Rajaraman, *Solitons and Instantons* (North Holland, Amsterdam, 1987).
 - [3] W. van Saarloos and P. C. Hohenberg, *Physica D* **56**, 303 (1992).
 - [4] R. Zwanzig, *Nonequilibrium Statistical Mechanics* (Oxford, New York, 2001).
 - [5] A. R. Fersht and V. Daggett, *Cell* **108**, 1 (2002).
 - [6] J. Halcrow, J. F. Gibson, P. Cvitanović, and D. Viswanath, *J. Fluid Mech.* **621**, 365 (2009).
 - [7] P. Holmes, J. L. Lumley, and G. Berkooz, *Turbulence, Coherent Structures, Dynamical Systems and Symmetry* (Cambridge University Press, Cambridge, 1998).
 - [8] G. Kawahara and S. Kida, *J. Fluid Mech.* **449**, 291 (2001).
 - [9] F. Noe, I. Horenko, C. Schutte, and J. C. Smith, *J. Chem. Phys.* **126**, 155102 (2007).
 - [10] J. Wang, J. Onuchic, and P. Wolynes, *Phys. Rev. Lett.* **76**, 4861 (1996).
 - [11] W.-J. Beyn, *IMA J. Numer. Anal.* **9**, 375 (1990).

- [12] J. W. Demmel, L. Dieci, and M. J. Friedman, *SIAM J. Sci. Comput.* **22**, 81 (2000).
- [13] E. J. Doedel and M. J. Friedman, *J. Comput. Appl. Math.* **26**, 155 (1989).
- [14] L. Liu, G. Moore, and R. D. Russell, *SIAM J. Sci. Comp.* **18**, 69 (1997).
- [15] Y. Liu, L. Liu, and T. Tang, *J. Comput. Phys.* **111**, 373 (1994).
- [16] A. F. Vakakis and M. F. A. Azeez, *Nonl. Dyn.* **15**, 245 (1998).
- [17] J. Hale and H. Koçak, *Dynamics and Bifurcations* (Springer-Verlag, New York, 1991).
- [18] J. K. Hale, L. A. Peletier, and W. C. Troy, *SIAM J. Appl. Math.* **61**, 102 (2000).
- [19] K. Nozaki and N. Bekki, *J. Phys. Soc. Japan* **53**, 1581 (1984).
- [20] J. Zinn-Justin, *Quantum Field Theory and Critical Phenomena* (Clarendon Press, Oxford, 2002).
- [21] L.-Y. Chen, N. Goldenfeld, and Y. Oono, *Phys. Rev. E* **54**, 376 (1996).
- [22] N. Goldenfeld, *Lectures on Phase Transitions and the Renormalization Group* (Addison-Wesley, Boston, 1993).
- [23] I. L. Egusquiza and M. A. V. Basagoiti, *Phys. Rev. A* **57**, 1586 (1998).
- [24] R. E. O'Malley, Jr, and E. Kirkinis, *Stud. Appl. Math.* **124**, 383 (2010).
- [25] T. Kunihiro, *Prog. Theor. Phys.* **97**, 179 (1997).
- [26] T. Kunihiro and J. Matsukidaira, *Phys. Rev. E* **57**, 4817 (1998).
- [27] T. Maruo, K. Nozaki, and A. Yosimori, *Prog. Theor. Phys.* **101**, 243 (1999).
- [28] H. Chiba, *J. Math. Phys.* **49**, 102703 (2008).
- [29] H. Chiba, *SIAM J. Appl. Dyn. Syst.* **8**, 1066 (2009).
- [30] S. H. Strogatz, *Nonlinear Dynamics and Chaos* (Perseus Publishing, Cambridge, Massachusetts, 2000).
- [31] F. Christiansen, P. Cvitanović, and V. Putkaradze, *Nonlinearity* **10**, 55 (1997).
- [32] Y. Kuramoto and T. Tsuzuki, *Prog. Theor. Phys.* **55**, 365 (1976).
- [33] G. I. Sivashinsky, *Acta Astr.* **4**, 1177 (1977).
- [34] L.-Y. Chen, N. Goldenfeld, and Y. Oono, *Phys. Rev. Lett.* **73**, 1311 (1994).
- [35] S.-I. Ei, K. Fujii, and T. Kunihiro, *Annal. Phys.* **280**, 236 (2000).
- [36] B. I. Cohen, J. A. Krommes, W. M. Tang, and M. N. Rosenbluth, *Nucl. Fusion* **16**, 971 (1972).
- [37] A. P. Hooper and R. Grimshaw, *Phys. Fluids* **28**, 37 (1985).
- [38] G. I. Sivashinsky and D. M. Michelson, *Prog. Theor. Phys. Suppl.* **66**, 2112 (1980).
- [39] P. Kent and J. Elgin, *Nonlinearity* **5**, 899 (1992).
- [40] R. W. Wittenberg and P. Holmes, *Chaos* **9**, 452 (1999).
- [41] T. S. Yang, *Physica D* **110**, 25 (1997).